

## Article

# A Role of Mineral Oxides on Trace Elements Behavior during Pulverized Coal Combustion

Ulung Muhammad Sutopo <sup>1</sup>, Erda Rahmilaila Desfitri <sup>2</sup>, Yukio Hayakawa <sup>1</sup>  and Shinji Kambara <sup>1,\*</sup> 

- <sup>1</sup> Environmental and Renewable Energy System Division, Graduate School of Engineering, Gifu University, Gifu 501-1193, Japan; z3921002@edu.gifu-u.ac.jp (U.M.S.); h\_yukio@gifu-u.ac.jp (Y.H.)
- <sup>2</sup> Chemical Engineering, Faculty of Industrial Engineering, Bung Hatta University, Padang 25133, Indonesia; rahmilaila01@gmail.com
- \* Correspondence: kambara@gifu-u.ac.jp; Tel.: +81-58-293-2581

**Abstract:** The issues of trace element emissions during coal combustion has been a concern in recent years due to their environmental pollutant. To study the trace element transformation, the thermodynamic calculation (FactSage 7.2) was used. Five kinds of pure mineral oxides ( $\text{Al}_2\text{O}_3$ ,  $\text{CaO}$ ,  $\text{Fe}_2\text{O}_3$ ,  $\text{K}_2\text{O}$ , and  $\text{MgO}$ ) and As, B, Cr, F, and Se in fly ash were considered for trace elements. The results confirm that all mineral oxides have a good correlation with arsenic to form  $\text{Ca}_3(\text{AsO}_4)_2$ ,  $\text{FeAsO}_4$ ,  $\text{K}_3\text{AsO}_4$ , and  $\text{Mg}_3(\text{AsO}_4)_2$ . Boron has a good relationship with Al, Ca, and Mg to form  $(\text{Al}_2\text{O}_3)_9(\text{B}_2\text{O}_3)_2$ ,  $\text{Ca}_3\text{B}_2\text{O}_6$ , and  $\text{Mg}_3\text{B}_2\text{O}_6$ . Chromium has a good correlation with K and Ca to form  $\text{K}_2\text{CrO}_4$ ,  $\text{CaCr}_2\text{O}_4$ . Furthermore,  $\text{FeF}_{3(s)}$ ,  $\text{KF}_{(s)}$ , and  $\text{AlF}_{3(s)}$  are predicted from the interaction of fluorine with  $\text{Fe}_2\text{O}_3$ ,  $\text{K}_2\text{O}$ , and  $\text{Al}_2\text{O}_3$ . The effect of mineral oxides on selenium partitioning are not observed. The inhibition order of trace elements by mineral oxides is as follow: As ( $\text{Al}_2\text{O}_3 > \text{MgO} > \text{CaO} > \text{Fe}_2\text{O}_3 > \text{K}_2\text{O}$ ), B ( $\text{Al}_2\text{O}_3$ ,  $\text{CaO}$ ,  $\text{Fe}_2\text{O}_3$ ,  $\text{K}_2\text{O}$ ,  $> \text{MgO}$ ), Cr ( $\text{CaO} > \text{K}_2\text{O} > \text{Al}_2\text{O}_3$ ,  $\text{MgO}$ ,  $\text{Fe}_2\text{O}_3$ ), F ( $\text{CaO} > \text{MgO} > \text{Al}_2\text{O}_3 > \text{Fe}_2\text{O}_3 > \text{K}_2\text{O}$ ). The results will be useful to control the trace element emissions.



**Citation:** Sutopo, U.M.; Desfitri, E.R.; Hayakawa, Y.; Kambara, S. A Role of Mineral Oxides on Trace Elements Behavior during Pulverized Coal Combustion. *Minerals* **2021**, *11*, 1270. <https://doi.org/10.3390/min11111270>

Academic Editor: Shifeng Dai

Received: 11 October 2021  
Accepted: 12 November 2021  
Published: 15 November 2021

**Publisher's Note:** MDPI stays neutral with regard to jurisdictional claims in published maps and institutional affiliations.



**Copyright:** © 2021 by the authors. Licensee MDPI, Basel, Switzerland. This article is an open access article distributed under the terms and conditions of the Creative Commons Attribution (CC BY) license (<https://creativecommons.org/licenses/by/4.0/>).

**Keywords:** coal fly ash; trace elements; combustion process; thermodynamic calculation

## 1. Introduction

According to the International energy agency, coal is still an important position as a world energy source during the next decade due to the perception that coal is the cheapest source and primary position in power generation [1]. In coal-thermal power generation, coal is used as raw material for energy production through the combustion process. The combustion of coal containing even only several parts per million of trace elements (TEs) could result in the release of several tons of pollutants into the environment [2]. The TEs in coal are defined as an element occurring in a very low amount (<100 ppm) [3,4]. The TEs introduced into a combustion system as part of the coal feeds or sorbents can only exit the combustion system through a finite number of pathways [5]. During the combustion process, many TEs such as As, Cd, Hg, Pb, and Se first vaporize and then condense either homogeneously to form submicron ash particles or heterogeneously to adsorb on the surface of fine fly ash particles which are hard to be captured by electrostatic precipitator, baghouse filter, and other air pollution control devices [6,7]. The issues of TEs emissions during coal combustion has been subjected to concern in recent years due to their environmental pollutant and technological problems during coal utilization for energy production. Lots of research has been studied the way to inhibit the release of easily volatilized TEs by the addition of sorbents, as summarized in Table 1.

**Table 1.** Literature on the ability of sorbents to inhibit the release of volatilized TEs.

Sorbents	Findings	Research
Kaoline	Addition of kaolin powders into the sewage sludge combustion contributed to inhibiting Pb and Cd compounds at the temperature of 1223 K due to the reaction of Pb and Cd compounds with the kaolin during combustion.	Yao et al., 2005 [8,9]
Activated carbon	Activated carbons can capture As and Se by the ash content of the activated carbon and the composition of the atmosphere.	López-Antón et al., (2007) [10]
Fly ash	Fly ash is an efficient sorbent for inhibiting As, Se, and Zn. Retention capacities of TEs depend on temperature and atmosphere.	Diza-Somoano et al., (2002) [11]
Limestone, Ca <sub>5</sub> O <sub>4</sub> , bauxite, kaolinite, and CaO	1. Absorbents can inhibit of TEs emissions. Kaolinite is the best for the sorption of Pb, bauxite for Cd, kaolinite, and bauxite have slight sorption on Cr, lime has no effect on Cr capture. 2. Combustion temperature influences the capture of TEs. The best temperature on the absorptive capacity was 1473 K. 3. The retention of As in fly ash is affected by CaO due to their chemical reaction.	Cheng et al., (2001), Gullett and Raghunathan (1994) [12,13]
Vanadium (V)	The correlation analysis between V and As give a coefficient $r = 58.7\%$ , Correlation among V and F ( $r = 31.6\%$ ) and B ( $r = 20.9\%$ ) is not significant.	Fiorentino et al., (2007) [14]
Titanium (Ti)	The nanostructured Ti flake surface can inhibit the release of some rare earth elements La, Lu, and Yb. Be recovery percentage was over 90%, while lanthanides have just a satisfactory recovery percentage (about 65% Yb and Lu and 50% La).	Barbulescu et al., 2019 [15]

It is necessary to understand TEs behavior during the coal combustion and gasification processes. Using the computation method of the thermodynamic equilibrium, lots of research has been studied TEs behavior and transformation during combustion and/or gasification process [16–23]. Liu et al. [21] investigated the effects of sewage sludge (SS) co-combustion conditions and interactions with Al<sub>2</sub>O<sub>3</sub>, CaO, Fe<sub>2</sub>O<sub>3</sub>, and SiO<sub>2</sub>. Their results show that in the SS co-combustion system with the multiple oxides of Al<sub>2</sub>O<sub>3</sub>, CaO, and SiO<sub>2</sub>, As reacted with Al<sub>2</sub>O<sub>3</sub> and CaO to form AlAsO<sub>4(s)</sub> and Ca<sub>3</sub>(AsO<sub>4</sub>)<sub>2(s)</sub> which in turn inhibited As volatilization. SiO<sub>2</sub> prevented As from reacting with CaO, thus decreasing Ca<sub>3</sub>(AsO<sub>4</sub>)<sub>2(s)</sub>. Shuqin Liu et al. [22] reported that the effect of mineral elements, the presence of K makes As less volatile due to the formation of K<sub>3</sub>AsO<sub>4</sub> and Se is not affected. Based on the results of lots of researches both in the experimental and thermodynamic study, it is clear that the emission of TEs during coal combustion is frequently controlled by the use of sorbents such as Al<sub>2</sub>O<sub>3</sub>, CaO, and K<sub>2</sub>O.

Mineral oxides are major elements present in fly ash, so understanding how TEs vapor interacts with these elements could lead the way to evaluate their use. Previous research narrowly focuses on calcium-based or carbon-based sorbents [10,11,24]. This paper presents the results of TEs vapor inhibition using five different kinds of mineral oxides. The experiments were carried out using the computation method of thermodynamic equilibrium (FactSage 7.2, Environmental and Renewable Energy Laboratory, Gifu University, Gifu, Japan). The effects of combustion temperature, mineral oxide type, and inhibition mechanism are tentatively determined. Applying these mineral oxides in the combustion process is a promising method to prevent trace element compounds into the environment and inhibit the release of the easily volatilized TEs.

## 2. Materials and Methods

### 2.1. Coal Fly Ash (CFA)

CFA was obtained from coal-fired power plants in Japan. The chemical properties of the CFA sample were determined based on X-ray fluorescence (XRF) analysis results (WDXRF S8 Tiger, Bruker AXS, Gifu, Japan), as shown in Table 2. In the sample, Al<sub>2</sub>O<sub>3</sub> is the higher mineral oxide contain (20.45%), followed by Fe<sub>2</sub>O<sub>3</sub> (15.65%), CaO (1.13%), K<sub>2</sub>O (1.06%), and MgO (0.61%). 12.53, 160, 7.7, 10, 3.87 mg/kg of As, B, Cr, F, and Se exist in the CFA sample, respectively.

**Table 2.** Chemical composition of CFA.

Main Oxides	Proportion (%)
SiO <sub>2</sub>	59.38
Al <sub>2</sub> O <sub>3</sub>	20.45
TiO <sub>2</sub>	0.62
Fe <sub>2</sub> O <sub>3</sub>	15.65
CaO	1.13
MgO	0.61
Na <sub>2</sub> O	0.47
K <sub>2</sub> O	1.06
P <sub>2</sub> O <sub>5</sub>	0.08
MnO	0.07
V <sub>2</sub> O <sub>5</sub>	0.01
SO <sub>3</sub>	0.49
Total	100
<b>Trace elements (mg/kg)</b>	
As	12.53
B	160.00
Cr	7.70
F	10.00
Se	3.87

## 2.2. FactSage: Thermodynamic Calculation

A thermodynamic calculation model used in this study was FactSage 7.2 software to make the thermodynamic calculation based on minimization of the Gibbs free energy. FactSage covers a compound database of all CFA components. Fiona et al. [25] reported that combining the mineral components (three major minerals: Al, Ca, and Fe) in samples (Victorian brown coal and Xin Jiang coal), Cr displayed excellent correlation with Al, while As has a good correlation with Ca. Following those results, in this study, five kinds of pure mineral oxides (Al<sub>2</sub>O<sub>3</sub>, CaO, Fe<sub>2</sub>O<sub>3</sub>, K<sub>2</sub>O, and MgO) and the major elements such as Al<sub>2</sub>O<sub>3</sub>, CaO, Fe<sub>2</sub>O<sub>3</sub>, SiO<sub>2</sub>, etc. in coal were considered for trace elements (As, B, Cr, F, and Se) in combustion process simulation. This calculation was used to predict the possible TEs-bearing compounds in CFA, their distribution, and the dominant interaction between minerals to each trace element. The data search used in this analysis includes FactPS and FToxid. The temperature selected for the simulation process range from 100 °C to 1600 °C and is performed in the combustion atmosphere condition. For calculations, 100 g of CFA was used to calculate the input data under pure oxygen combustion conditions. Firstly, equilibrium composition was determined for trace elements individually, with 3% addition of each mineral oxides (Al<sub>2</sub>O<sub>3</sub>, CaO, Fe<sub>2</sub>O<sub>3</sub>, and K<sub>2</sub>O and, MgO), then the calculation was determined for each trace element, with the major components present in the original CFA. All the input reactant temperature was 25 °C at atmospheric conditions. During simulation analysis, gases and solid species are chosen as output.

## 3. Results

### 3.1. Trace Elements Interaction with Mineral Oxide

The thermodynamic equilibrium calculations were conducted to predict the possible interactions between TEs and mineral oxides. The TEs distribution by the effect of adding mineral oxides during combustion at temperature range 100–1600 °C were shown in Figures 1–5 and Table 3, respectively. As shown in Figure 1a–e, As and mineral oxides (Al, Ca, Fe, K, and Mg) interact to form new species including AlAsO<sub>4</sub>, Ca<sub>3</sub>(AsO<sub>4</sub>)<sub>2</sub>, FeAsO<sub>4</sub>, K<sub>3</sub>AsO<sub>4</sub>, and Mg<sub>3</sub>(AsO<sub>4</sub>)<sub>2</sub> with a small contribution of gaseous species such as AsO and As<sub>4</sub>O<sub>6</sub>. Many studies have confirmed that As was associated with both organic matter and inorganic minerals (clay minerals, sulfides). Figure 1a–e, indicates that all mineral oxides can minimize the release of emission.

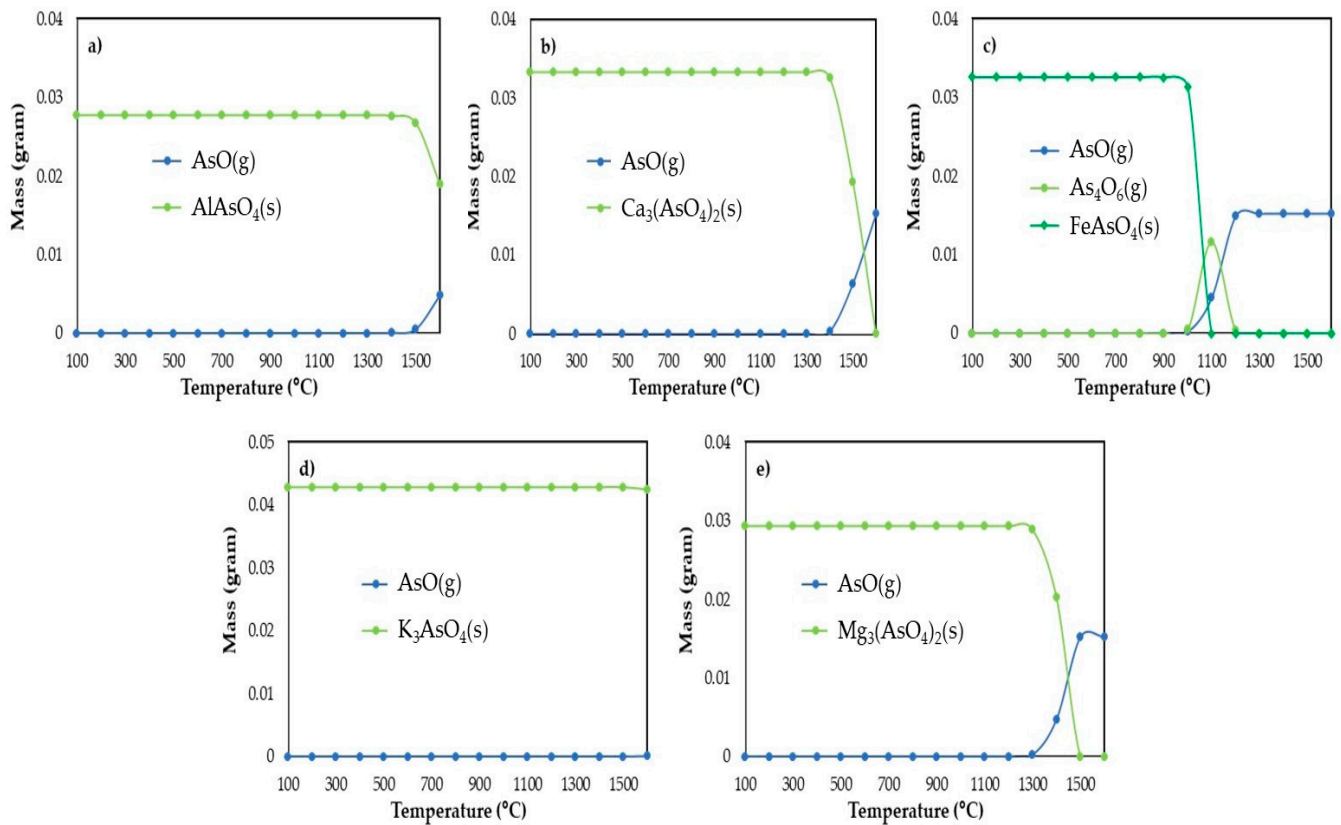


**Figure 1.** Equilibrium composition of As-Mineral oxides interactions during combustion: (a) As-O<sub>2</sub>-Al<sub>2</sub>O<sub>3</sub>; (b) As-O<sub>2</sub>-CaO; (c) As-O<sub>2</sub>-Fe<sub>2</sub>O<sub>3</sub>; (d) As-O<sub>2</sub>-K<sub>2</sub>O; (e) As-O<sub>2</sub>-MgO.

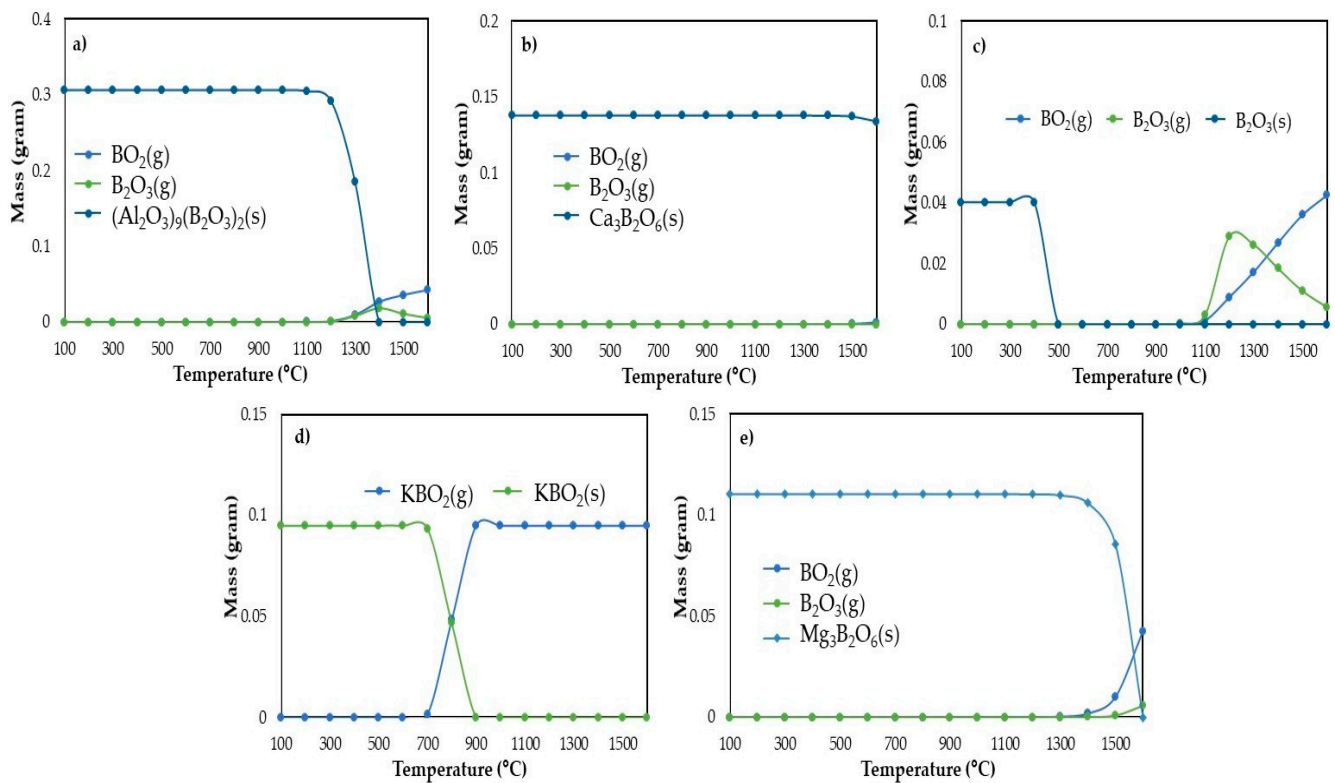


**Figure 2.** Equilibrium composition of B-Mineral oxides interactions during combustion: (a) B-O<sub>2</sub>-Al<sub>2</sub>O<sub>3</sub>; (b) B-O<sub>2</sub>-CaO; (c) B-O<sub>2</sub>-Fe<sub>2</sub>O<sub>3</sub>; (d) B-O<sub>2</sub>-K<sub>2</sub>O, and (e) B-O<sub>2</sub>-MgO.

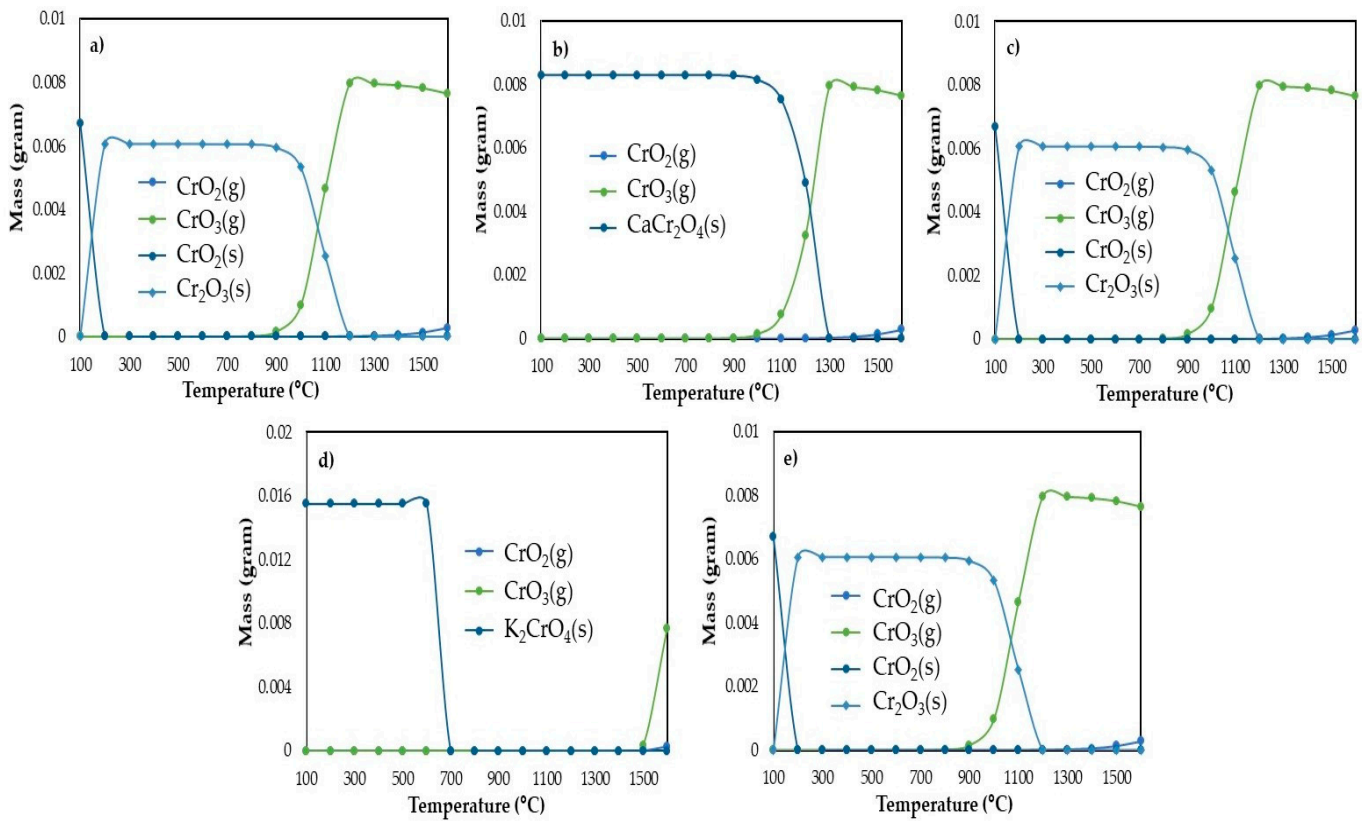


**Figure 3.** Equilibrium composition of Cr-Mineral oxides interactions during combustion: (a) Cr-O<sub>2</sub>-Al<sub>2</sub>O<sub>3</sub>; (b) Cr-O<sub>2</sub>-CaO; (c) Cr-O<sub>2</sub>-Fe<sub>2</sub>O<sub>3</sub>; (d) Cr-O<sub>2</sub>-K<sub>2</sub>O, and (e) Cr-O<sub>2</sub>-MgO.

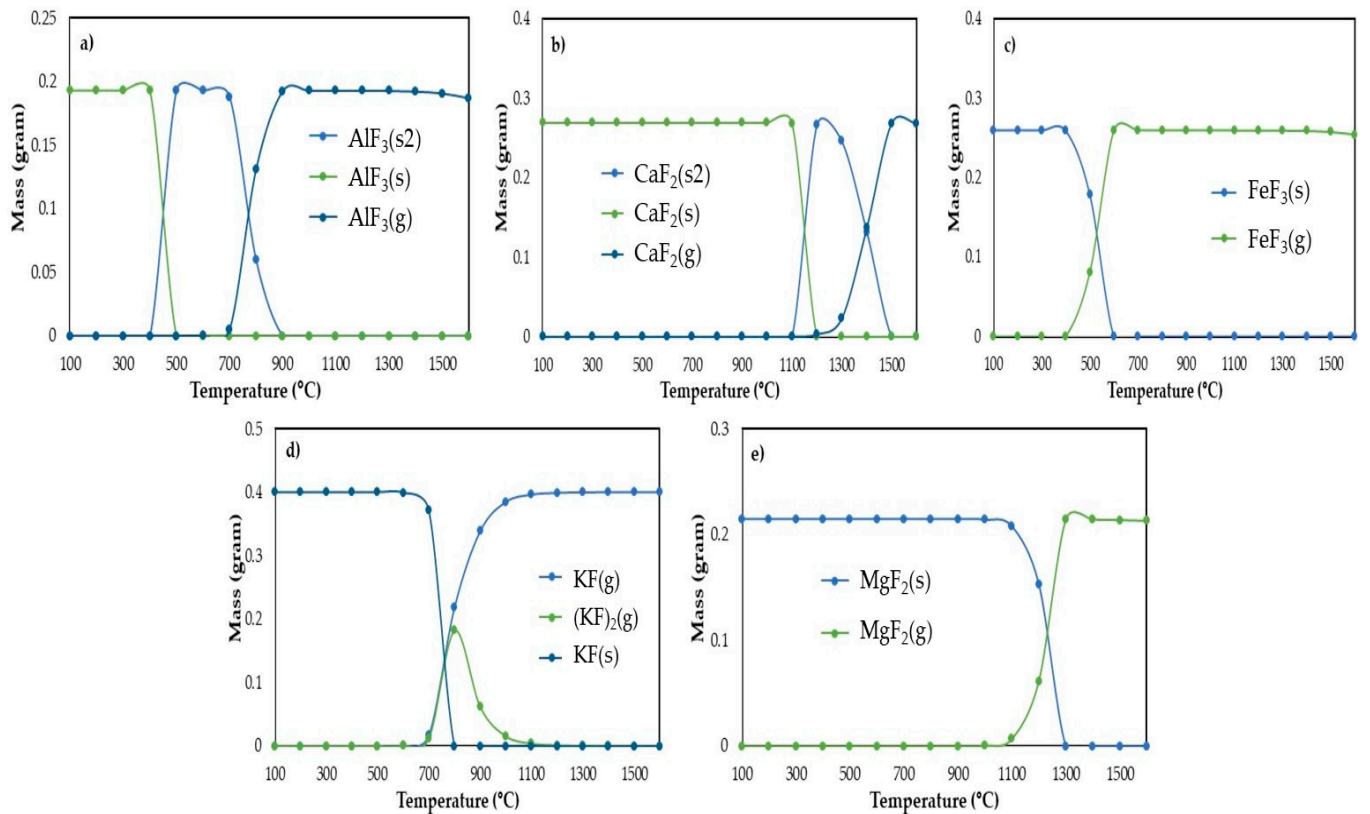


**Figure 4.** Equilibrium composition of F-Mineral oxides interactions during combustion: (a) F-O<sub>2</sub>-Al<sub>2</sub>O<sub>3</sub>; (b) F-O<sub>2</sub>-CaO; (c) F-O<sub>2</sub>-Fe<sub>2</sub>O<sub>3</sub>; (d) F-O<sub>2</sub>-K<sub>2</sub>O, and (e) F-O<sub>2</sub>-MgO.

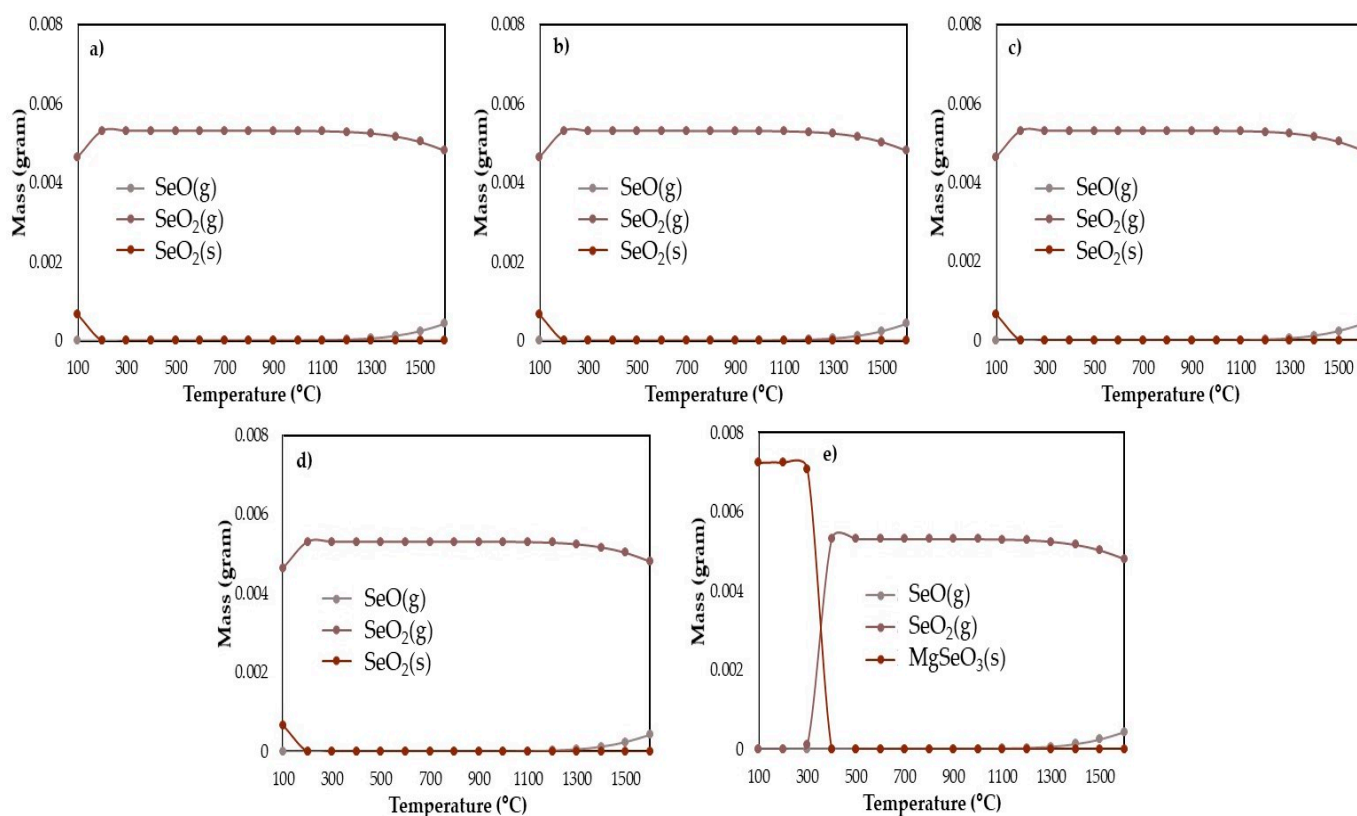


**Figure 5.** Equilibrium composition of Se-Mineral oxides interactions during combustion: (a) Se-O<sub>2</sub>-Al<sub>2</sub>O<sub>3</sub>; (b) Se-O<sub>2</sub>-CaO; (c) Se-O<sub>2</sub>-Fe<sub>2</sub>O<sub>3</sub>; (d) Se-O<sub>2</sub>-K<sub>2</sub>O, and (e) Se-O<sub>2</sub>-MgO.

**Table 3.** Prediction of the main species during the interaction of trace elements with mineral oxide during the combustion process.

Component Interactions	Formed Species				
	As	B	Cr	F	Se
TEs-O <sub>2</sub> -K	K <sub>3</sub> AsO <sub>4</sub> (s)	KBO <sub>2</sub> (s)	K <sub>2</sub> CrO <sub>4</sub> (s)	KF(s)	SeO <sub>2</sub> (s)
TEs-O <sub>2</sub> -Ca	Ca <sub>3</sub> (AsO <sub>4</sub> ) <sub>2</sub> (s)	Ca <sub>3</sub> B <sub>2</sub> O <sub>6</sub> (s)	CaCr <sub>2</sub> O <sub>4</sub> (s)	CaF <sub>2</sub> (s)	SeO <sub>2</sub> (s)
TEs-O <sub>2</sub> -Al	AlAsO <sub>4</sub> (s)	(Al <sub>2</sub> O <sub>3</sub> ) <sub>9</sub> (B <sub>2</sub> O <sub>3</sub> ) <sub>2</sub> (s)	CrO <sub>2</sub> (s)	AlF <sub>3</sub> (s)	SeO <sub>2</sub> (s)
TEs-O <sub>2</sub> -Fe	FeAsO <sub>4</sub> (s)	B <sub>2</sub> O <sub>3</sub> (s)	CrO <sub>2</sub> (s)	FeF <sub>3</sub> (s)	SeO <sub>2</sub> (s)
TEs-O <sub>2</sub> -Mg	Mg <sub>3</sub> (AsO <sub>4</sub> ) <sub>2</sub> (s)	Mg <sub>3</sub> B <sub>2</sub> O <sub>6</sub> (s)	CrO <sub>2</sub> (s)	MgF <sub>2</sub> (s)	MgSeO <sub>3</sub> (s)

During coal combustion, B has a good relationship with Al, Ca, and Mg, which are important for the reaction with B to form (Al<sub>2</sub>O<sub>3</sub>)<sub>9</sub>(B<sub>2</sub>O<sub>3</sub>)<sub>2</sub>, Ca<sub>3</sub>B<sub>2</sub>O<sub>6</sub>, and Mg<sub>3</sub>B<sub>2</sub>O<sub>6</sub> in the temperature in the range 100–1400 °C and transform into BO<sub>2</sub> and B<sub>2</sub>O<sub>3</sub> in gaseous species with temperature increases (except the interaction with Ca).

The effect of mineral oxides on Cr, the presence of Ca and K make Cr less volatile due to the formation of CaCr<sub>2</sub>O<sub>4</sub> and K<sub>2</sub>CrO<sub>4</sub>, and the effect of Al<sub>2</sub>O<sub>3</sub>, Fe<sub>2</sub>O<sub>3</sub>, MgO is not affected on Cr as shown in Figure 3a–e. The interaction of Al<sub>2</sub>O<sub>3</sub>, Fe<sub>2</sub>O<sub>3</sub>, MgO were introduced on Cr. At T > 1100 °C, CrO<sub>3</sub>(g) was formed and became the main gaseous species with a small contribution of CrO<sub>2</sub>(g). At T < 1200 °C, Cr<sub>2</sub>O<sub>3</sub> and CrO<sub>2</sub> were formed in the solid phase. Cr becomes volatile only at high combustion temperatures, and gaseous species leave the combustion zone and cooling condition [20,22].

The FeF<sub>3</sub>(s), KF(s), and AlF<sub>3</sub>(s) are predicted in equilibrium calculations from the interaction of F and Al<sub>2</sub>O<sub>3</sub>, Fe<sub>2</sub>O<sub>3</sub>, and K<sub>2</sub>O in low-temperature combustion (<700 °C) as shown in Figure 4a,c,d and then transforms into AlF<sub>3</sub>(g), FeF<sub>3</sub>(g), and KF(g) with the temperature increase. The presence of Ca and Mg make F less volatile due to the formation of CaF<sub>2</sub> and MgF<sub>2</sub> events in high-temperature combustions (T = 1100–1200 °C). Wang et al. [26]

reported that mainly F compound in coal is insoluble fluoride such as  $\text{AlF}_3$ ,  $\text{CaF}_2$ ,  $\text{FeF}_3$ , and  $\text{MgF}$ . These fluorides are the main occurrence state after the coal combustion process and are difficult to break down even at high temperatures.

The effect of mineral oxides on Se are different from other TEs. Figure 5a–e, Se forms in the gas phase almost over the whole range of temperatures (i.e.,  $\text{SeO}$  and  $\text{SeO}_2$ ). The Se can be endured in the gas phase even at temperatures lower than  $200\text{ }^\circ\text{C}$ . The effect of Al, Ca, Fe, and K on Se partitioning are not observed. On the other hand, the interaction of Se with  $\text{MgO}$  promotes the formation of  $\text{MgSeO}_3$  at temperatures  $100\text{--}300\text{ }^\circ\text{C}$  as shown in Figure 5e. As reported, almost all of the Se was presented as the vaporized  $\text{SeO}$  and  $\text{SeO}_2$ . Note that solid  $\text{SeO}_2$  has a vapor pressure even than its sublimation temperature ( $590\text{ K}$  at  $1\text{ atm}$ ). This means that a small amount of  $\text{SeO}_2$  can stay even at the terminal side of the gas cooling process, and then the nucleation might be more dominant than the deposition on other entrained particles during the phase change of  $\text{SeO}_2$  [27].

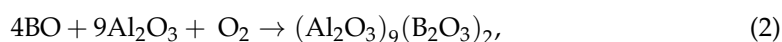
### 3.2. Trace Element Interactions with Coal Fly Ash Components

Arsenic-CFA interaction favors the formation of arsenates such as  $\text{AlAsO}_4$ ,  $\text{Ca}_3(\text{AsO}_4)_2$ ,  $\text{K}_3\text{AsO}_4$ , and gaseous arsenate such as  $\text{AsO}$ ,  $\text{As}_2\text{O}_3$ ,  $\text{As}_4\text{O}_6$ , etc. All the main CFA components (Al, Ca, Fe, K, Mg, Mn, Na, P, S, Si, Ti, and V) interaction have been introduced in the input calculation to study which are the dominant interaction with As, and it can be seen from Figure 6a. In that case, As is predicted to form  $\text{AlAsO}_4$ . When the temperature is higher than  $1400\text{ }^\circ\text{C}$ , a small amount of  $\text{AsO}_{(g)}$  appears and the formation of  $\text{AlAsO}_{4(s)}$  is decreased to the final temperature of the combustion process, indicating that  $\text{AlAsO}_{4(s)}$  is the arsenate species form during the combustion process. The mechanism process can be explained according to the following Equation (1).



Although Si as  $\text{SiO}_2$  is the highest percentage component in CFA ash samples, the presence of Al as  $\text{Al}_2\text{O}_3$  inhibits the effect of the other components on the formation of TEs-bearing species during the combustion process. This result is in line with Liu et al. [21]  $\text{Al}_2\text{O}_3$  reacted more easily than  $\text{CaO}$ ,  $\text{Fe}_2\text{O}_3$ , and  $\text{SiO}_2$  and related to the reactivity of the oxides, the order of the reactivity of the oxides with As was thus:  $\text{Al}_2\text{O}_3 > \text{CaO} > \text{Fe}_2\text{O}_3 > \text{SiO}_2$ . Roy et al. [23] reported that the equilibrium distribution of As during oxy-fuel combustion of three Victorian brown coals at different temperatures, almost all the As was found to present as  $\text{As}_2\text{O}_{3(s)}$ ,  $\text{Ca}_3(\text{AsO}_4)_2(s)$ , and  $\text{As}_4\text{O}_{6(g)}$ .

Boron-CFA ash interaction,  $(\text{Al}_2\text{O}_3)_9(\text{B}_2\text{O}_3)_2$  is predicted as the most probable species forming resulting from B-main CFA components interaction at a temperature below  $1400\text{ }^\circ\text{C}$  with a small contribution of gaseous boron such as  $\text{BO}$ ,  $\text{BO}_2$ ,  $\text{B}_2\text{O}_3$ ,  $\text{NaBO}_2$ , and  $\text{KBO}_2$ . The mechanism process can be explained according to the following Equation (2).



In the case of Cr, the main coal and Cr interaction, the Cr compounds preferentially formed are,  $\text{CrO}_{3(g)}$  ( $T > 1200\text{ }^\circ\text{C}$ ),  $\text{Cr}_2\text{O}_{3(s)}$  ( $T = 200\text{--}1100\text{ }^\circ\text{C}$ ),  $\text{CrO}_{2(g)}$  ( $T > 1400\text{ }^\circ\text{C}$ ) and  $\text{CrO}_{2(s)}$  ( $T < 200\text{ }^\circ\text{C}$ ).  $\text{CrO}_2$  in the solid phase is predicted to be chromate species consistent in the CFA. The mechanism process can be explained according to the following Equation (3).



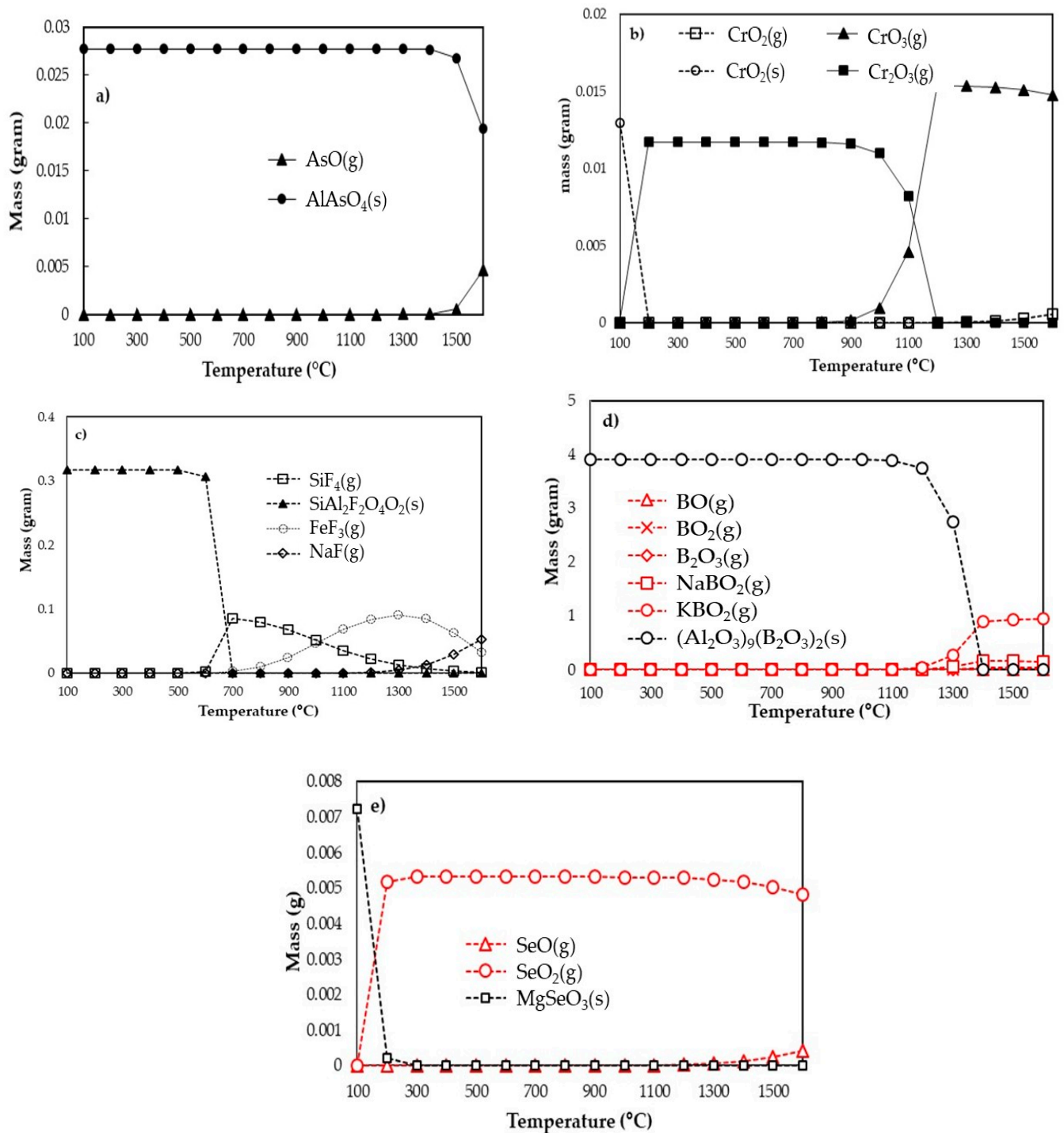
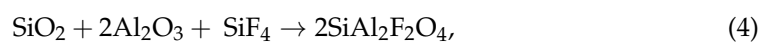


**Figure 6.** Equilibrium composition of TEs-Coal fly ash components interaction: (a) arsenic; (b) chromium; (c) fluorine; (d) boron, and (e) selenium.

During the combustion process, F is predicted to form mostly gaseous oxide and fluoride. Figure 6c, at the highest temperature,  $\text{SiF}_4(\text{g})$ ,  $\text{FeF}_3(\text{g})$  and  $\text{NaF}(\text{g})$  in the gaseous phase were the dominant species forming during interaction of F and fly ash components and  $\text{SiAl}_2\text{F}_2\text{O}_4(\text{s})$  was formed at temperature  $<700^\circ\text{C}$ . The mechanism process can be explained according to the following Equation (4).



Selenium compounds are present during the combustion process in the gas phases (SeO and SeO<sub>2</sub>) at the highest temperature. As shown in Figure 6e and Table 3, Se is predicted to form gaseous oxide and selenite. SeO<sub>2</sub> is predicted to be the dominant species over the entire temperature range studied with a small contribution of SeO. At temperatures below 300 °C, MgSeO<sub>3</sub> in solid-phase starts to form, which results in a small drop in the SeO and SeO<sub>2</sub> compound, and MgSeO<sub>3</sub> is the selenite species contained in coal. The mechanism process can be explained according to the following Equation (5).



#### 4. Discussion

##### 4.1. The Migration of Trace Elements during Combustion Process

According to the above results, the interactions of trace elements with CFA components and/or mineral oxides may reduce the emission of gaseous TEs due to the formation of thermally stable TEs such as ash arsenates as shown in Equations (1)–(5). During the combustion process, mineral oxides make the TEs less volatile due to the formation of a complex compound of TEs and releasing the TEs emissions as tabulated in Table 4. The releasing of As emission formed at higher temperature (T > 1400 °C), B emission at T > 1100 °C, Cr emission at T > 1000 °C, F emission at T > 600 °C, and the most volatile are Se at T > 200 °C.

**Table 4.** Prediction of the species during the interaction of trace elements with CFA during the combustion process.

Interaction	Species of Trace Elements Produced	
	Gaseous	Solid
Arsenic (As)	As, As <sub>2</sub> , As <sub>3</sub> , As <sub>4</sub> , AsN, AsO, As <sub>2</sub> O <sub>3</sub> , As <sub>4</sub> O <sub>6</sub> , AsS, As <sub>4</sub> S <sub>4</sub>	AlAsO <sub>4</sub> , K <sub>3</sub> AsO <sub>4</sub> , Ca <sub>3</sub> (AsO <sub>4</sub> ) <sub>2</sub>
Boron (B)	B <sup>-</sup> , B, B <sup>+</sup> , B <sub>2</sub> , BN, BO, B <sub>2</sub> O, BO <sub>2</sub> <sup>-</sup> , BO <sub>2</sub> , (BO) <sub>2</sub> , B <sub>2</sub> O <sub>3</sub> , NaBO <sub>2</sub> , AlBO <sub>2</sub> , BS, B <sub>2</sub> S <sub>2</sub> , B <sub>2</sub> S <sub>3</sub> , KBO <sub>2</sub>	(Al <sub>2</sub> O <sub>3</sub> ) <sub>9</sub> (B <sub>2</sub> O <sub>3</sub> ) <sub>2</sub> , Mg <sub>2</sub> B <sub>2</sub> O <sub>5</sub> , (CaO) <sub>2</sub> (Al <sub>2</sub> O <sub>3</sub> )(B <sub>2</sub> O <sub>3</sub> ), Mg <sub>3</sub> B <sub>2</sub> O <sub>6</sub> , Ca <sub>11</sub> B <sub>2</sub> Si <sub>4</sub> O <sub>22</sub>
Chromium (Cr)	Cr, Cr <sup>-</sup> , Cr <sup>+</sup> , CrN, CrO, CrO <sub>2</sub> , CrO <sub>3</sub> , CrS	CrO <sub>2</sub> , Cr <sub>2</sub> O <sub>3</sub> , K <sub>2</sub> CrO <sub>4</sub> , Ca <sub>3</sub> Cr <sub>2</sub> Si <sub>3</sub> O <sub>12</sub>
Fluorine (F)	F <sup>-</sup> , F, OF, O <sub>2</sub> F, ONF, NaF, (NaF) <sub>2</sub> , MgF, MgF <sub>2</sub> , AlF, AlF <sub>3</sub> , AlF <sub>4</sub> <sup>-</sup> , OAlF, OAlF <sub>2</sub> <sup>-</sup> , NaAlF <sub>4</sub> , SiF <sub>4</sub> , OSiF <sub>2</sub> , KF, (KF) <sub>2</sub> , KAlF <sub>4</sub> , CaF <sub>2</sub> , TiF <sub>3</sub> , OTiF, OTiF <sub>2</sub> , FeF, FeF <sub>2</sub> , FeF <sub>3</sub>	SiAl <sub>2</sub> F <sub>2</sub> O <sub>4</sub> , Mg <sub>3</sub> SiF <sub>2</sub> O <sub>4</sub> , Mg <sub>5</sub> Si <sub>2</sub> F <sub>2</sub> O <sub>8</sub> , CaF <sub>2</sub> , Ca <sub>4</sub> Si <sub>2</sub> F <sub>2</sub> O <sub>7</sub> , Ca <sub>12</sub> Al <sub>14</sub> F <sub>2</sub> O <sub>32</sub> , Ca <sub>5</sub> Si <sub>2</sub> F <sub>2</sub> O <sub>8</sub>
Selenium (Se)	Se, Se <sub>2</sub> , Se <sub>3</sub> , Se <sub>4</sub> , Se <sub>5</sub> , Se <sub>6</sub> , Se <sub>7</sub> , Se <sub>8</sub> , SeO, SeO <sub>2</sub> , NSe, AlSe, Al <sub>2</sub> Se, SiSe, SiSe <sub>2</sub> , SeS, TiSe	MgSeO <sub>3</sub>

##### 4.2. Trace Element Inhibition Characteristic during Combustion Process

Some of the researchers have confirmed that the migration of TEs is influenced by the combustion parameter, concentration, flue gas component, occurrence state in coal, volatility of trace element compounds, etc. [28,29]. Combustion temperature as a combustion parameter affected the inhibition of TEs. Figure 7 shows the trace element inhibition function of adding different mineral oxides (CaO, MgO, K<sub>2</sub>O, Al<sub>2</sub>O<sub>3</sub>, and Fe<sub>2</sub>O<sub>3</sub>) under combustion temperature at 400, 800, and 1200 °C atmospheric conditions. From Figure 7a, the arsenic inhibition ratio was observed at 400 °C as a function of adding mineral oxides was 100% for each kind of mineral oxides. In the temperature studied 400, 800, and 1200 °C, the inhibition of arsenic by CaO, MgO, K<sub>2</sub>O, Al<sub>2</sub>O<sub>3</sub>, and Fe<sub>2</sub>O<sub>3</sub> decreased from 100 to 42.64 to 42.64%, 100 to 59.34 to 59.34%, 100 to 25.39 to 25.38%, 100 to 70.37 to 70.37%, and 100 to 44.93 to 0%, respectively. As temperature increases, the inhibition of arsenic was decrease as follow: T = 800 °C Al<sub>2</sub>O<sub>3</sub> > MgO > Fe<sub>2</sub>O<sub>3</sub> > CaO > K<sub>2</sub>O, T = 1200 °C Al<sub>2</sub>O<sub>3</sub> > MgO > CaO > K<sub>2</sub>O > Fe<sub>2</sub>O<sub>3</sub>. The results show that the inhibition ratio of Al<sub>2</sub>O<sub>3</sub> was higher than other mineral oxides in each temperature range. Comparing the effect of combustion temperatures, the best condition given by at T = 800 °C. As reported by Chen et al. [30] the inhibition of As was affected by the adsorption temperatures. The inhibition of As was enhanced with temperature increasing (T = from 573 to 723 K). However, less As was captured by CaO at a lower temperature (T = 573 K) and higher temperatures (T = 1173 K

and 1323 K). Han et al. [31] also reported, CaO inhibited the As releasing more effectively than Fe<sub>2</sub>O<sub>3</sub> at 723 K. However, when it reached higher temperatures (T > 973 K), CaO did not show more excellent inhibitory effects than Fe<sub>2</sub>O<sub>3</sub> due to sulfur dioxide formed and competes with As<sub>2</sub>O<sub>3</sub> to react with CaO which would obstruct the inhibition of As<sub>2</sub>O<sub>3</sub> by CaO. Zhang et al. [32] suggest that Ca and Fe provide reactive sites and act as a catalyst and reactant in the inhibition processes. Physisorption may be the main As inhibition mechanism for Al<sub>2</sub>O<sub>3</sub> due to the great surface area, which suggests that the great surface area may provide more active sites for gaseous arsenic [32,33]. Comparing the surface area of Al<sub>2</sub>O<sub>3</sub>, CaO, Fe<sub>2</sub>O<sub>3</sub>, and MgO the surface area of MgO (~90 m<sup>2</sup>/g), Al<sub>2</sub>O<sub>3</sub> (87.19 m<sup>2</sup>/g) was higher than Fe<sub>2</sub>O<sub>3</sub> (12.19 m<sup>2</sup>/g) and CaO (8.91 m<sup>2</sup>/g) [32,34]. Mineral oxides on the surface of activated carbon can act as a catalyst in the inhibition process, indicating that Al provides a large number of reactive sites per unit mass relative to Ca and Fe.

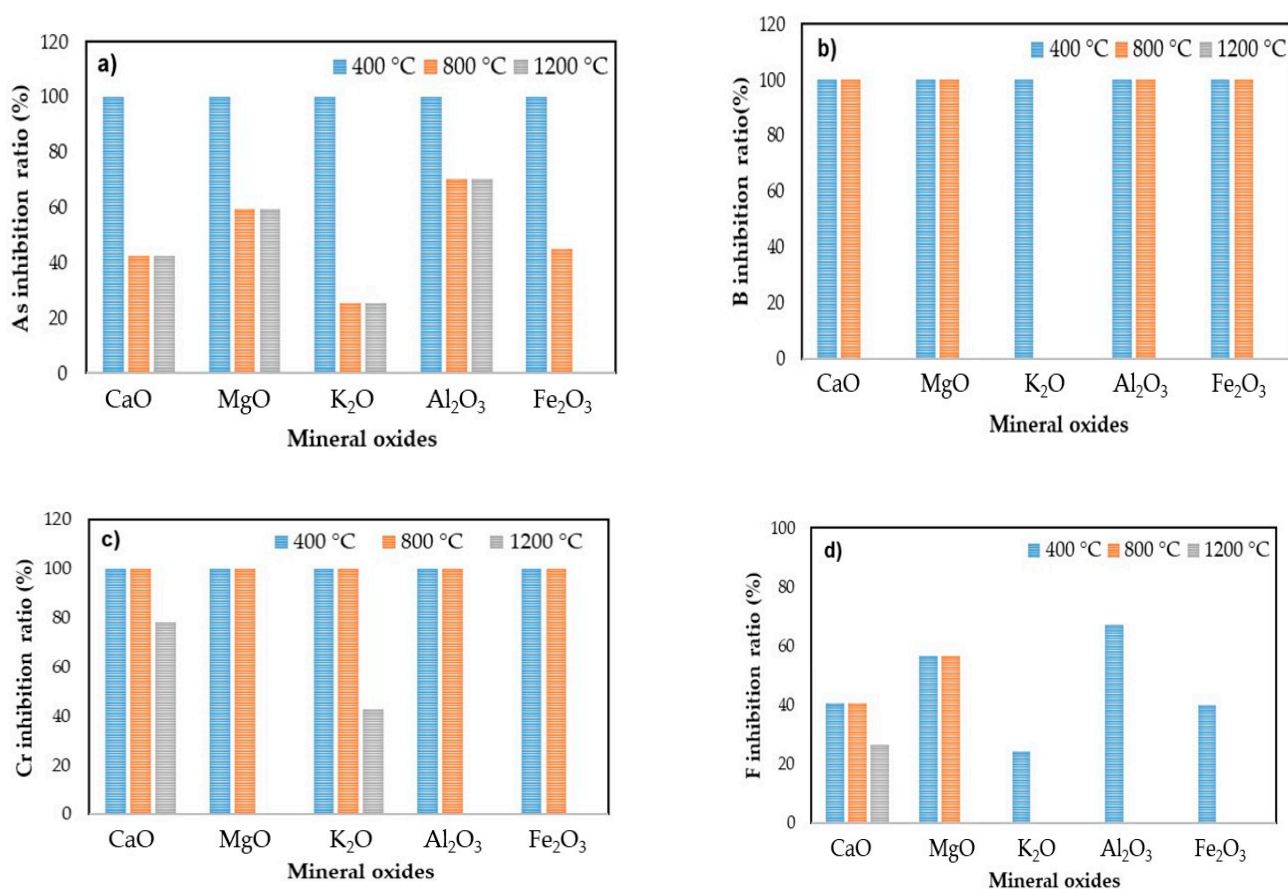


**Figure 7.** Impact of addition of mineral oxides on trace elements (TEs) inhibition during combustion at T = 400 °C, 800 °C, and 1200 °C; (a) arsenic; (b) boron; (c) chromium, and (d) fluorine.

The inhibition ratio of B at temperature 400–800 °C by Al<sub>2</sub>O<sub>3</sub>, CaO, Fe<sub>2</sub>O<sub>3</sub>, K<sub>2</sub>O, and MgO were 100% (except for K<sub>2</sub>O at T = 800 °C, the inhibition ratio was 0%) when the combustion temperature is further increased to 1200 °C, the inhibition ratio was 0% as shown in Figure 7b. The inhibition ratio of Cr shows almost the same behavior as B at temperature 400–800 °C for all mineral oxides. When the temperature reaches 1200 °C, only CaO and K<sub>2</sub>O can inhibit Cr release during combustion as shown in Figure 7c.

For fluorine, the inhibition ratio at temperature 400 °C, again Al<sub>2</sub>O<sub>3</sub> shows more effectively than other mineral oxides. The fluorine inhibition by Al<sub>2</sub>O<sub>3</sub>, CaO, Fe<sub>2</sub>O<sub>3</sub>, K<sub>2</sub>O, and MgO accounts for 40.66%, 56.57%, 24.20, 67.08%, and 39.70%, respectively. When the temperature reaches 800 °C, only CaO and MgO can inhibit F release with the inhibition rate were 40.66% and 56.57% and at temperature increase to 1200 °C, only CaO can inhibit F release during the combustion as shown in Figure 7d (inhibition ratio decreases to 26.31%).

On the other hand, different results pattern was investigated for Se. All the mineral oxides at all temperatures studied did not show inhibitory effects to Se during the combustion process. As mentioned before, almost all of the Se was presented as the vaporized SeO and SeO<sub>2</sub> during coal combustion conditions.

The inhibition order of TEs during combustion is as follow: As (Al<sub>2</sub>O<sub>3</sub> > MgO > CaO > Fe<sub>2</sub>O<sub>3</sub> > K<sub>2</sub>O), B (Al<sub>2</sub>O<sub>3</sub>, CaO, Fe<sub>2</sub>O<sub>3</sub>, K<sub>2</sub>O, > MgO), Cr (CaO > K<sub>2</sub>O > Al<sub>2</sub>O<sub>3</sub>, MgO, Fe<sub>2</sub>O<sub>3</sub>), and F (CaO > MgO > Al<sub>2</sub>O<sub>3</sub>, > Fe<sub>2</sub>O<sub>3</sub> > K<sub>2</sub>O). Based on the discussion above, mineral oxides and temperature have an important role in the migration of TEs during the combustion process. This condition is because mineral oxides have a negative charge and a high surface-to-volume ratio. Otherwise, trace elements have a positive charge, adsorbed on their surface [35]. In coal combustion and gasification processes, ash deposits are formed on the heat-absorbing surfaces of the exposed process equipment. Ash fusion temperatures (AFTs) are the important characteristics of the coal ashes and signify the temperature range over which the ash deposits are formed on the heat absorbing surfaces of the process equipment [36].

## 5. Conclusions

The distribution and transformation mechanism of As, B, Cr, F, and Se in CFA during the combustion process based on thermodynamic calculation was investigated. During coal combustion, all mineral oxides correlate with As to form Ca<sub>3</sub>(AsO<sub>4</sub>)<sub>2</sub>, FeAsO<sub>4</sub>, K<sub>3</sub>AsO<sub>4</sub>, and Mg<sub>3</sub>(AsO<sub>4</sub>)<sub>2</sub> with a small contribution of gaseous species such as AsO and As<sub>4</sub>O<sub>6</sub>. B has a good relationship with Al, Ca, and Mg to form (Al<sub>2</sub>O<sub>3</sub>)<sub>9</sub>(B<sub>2</sub>O<sub>3</sub>)<sub>2</sub>, Ca<sub>3</sub>B<sub>2</sub>O<sub>6</sub>, and Mg<sub>3</sub>B<sub>2</sub>O<sub>6</sub> in the temperature in range 100–1400 °C. The effect of mineral oxides on Cr, the presence of Ca and K make Cr less volatile due to the formation of CaCr<sub>2</sub>O<sub>4</sub> and K<sub>2</sub>CrO<sub>4</sub>, the effect of Al<sub>2</sub>O<sub>3</sub>, Fe<sub>2</sub>O<sub>3</sub>, MgO is not affected on Cr. The AlF<sub>3(s)</sub>, FeF<sub>3(s)</sub>, and KF<sub>(s)</sub> are predicted in equilibrium calculations from the interaction of F with Al<sub>2</sub>O<sub>3</sub>, Fe<sub>2</sub>O<sub>3</sub>, and K<sub>2</sub>O in low-temperature combustion (<700 °C) and then transforms into AlF<sub>3(g)</sub>, FeF<sub>3(g)</sub>, and KF<sub>(g)</sub>, with the temperature increase. The effect of Al, Ca, Fe, and K on Se partitioning are not observed, almost all of the Se was presented as the vaporized SeO and SeO<sub>2</sub>. The interaction of Se with MgO promotes the formation of MgSeO<sub>3</sub> at temperature 100–300 °C. The results confirm that the interaction between mineral oxides and gaseous trace elements promotes the formation of stable TEs such as arsenate, fluoride, etc. This is because mineral oxides have a negative charge, a high surface-to-volume ratio, otherwise, trace elements are usually with a positive charge, adsorbed on its surface. The inhibition order of trace elements by mineral oxides during combustion is as follow: As (Al<sub>2</sub>O<sub>3</sub> > MgO > CaO > Fe<sub>2</sub>O<sub>3</sub> > K<sub>2</sub>O), B (Al<sub>2</sub>O<sub>3</sub>, CaO, Fe<sub>2</sub>O<sub>3</sub>, K<sub>2</sub>O, > MgO), Cr (CaO > K<sub>2</sub>O > Al<sub>2</sub>O<sub>3</sub>, MgO, Fe<sub>2</sub>O<sub>3</sub>), and F (CaO > MgO > Al<sub>2</sub>O<sub>3</sub>, > Fe<sub>2</sub>O<sub>3</sub> > K<sub>2</sub>O). As and B have a good correlation with Al<sub>2</sub>O<sub>3</sub>, while Cr and F with CaO.

**Author Contributions:** Conceptualization, S.K.; methodology, S.K.; software, U.M.S.; validation, U.M.S.; formal analysis, U.M.S., E.R.D. and Y.H.; investigation, U.M.S., E.R.D. and Y.H.; resources, S.K.; data curation, U.M.S., E.R.D., Y.H. and S.K.; writing—original draft preparation, U.M.S.; writing—review and editing, U.M.S., E.R.D., Y.H. and S.K.; visualization, U.M.S. and S.K.; supervision, S.K.; project administration, S.K.; funding acquisition, S.K. All authors have read and agreed to the published version of the manuscript.

**Funding:** This research was funded by TOHOKU ELECTRIC POWER COMPANY.

**Data Availability Statement:** All data are contained within the article.

**Acknowledgments:** The experiments in this research were conducted in the lab Environmental and Renewable Energy (Kambara Laboratory). We would like to thank all Kambara laboratory members for their kind help in our experiments and TOHOKU ELECTRIC POWER COMPANY for financial support.

**Conflicts of Interest:** The authors declare no conflict of interest.

## References

1. International Energy Agency, Coal Report; Coal 2020 Analysis and Forecast to 2025. Available online: <http://www.iea.org/reports/coal-2020/demand> (accessed on 15 April 2021).
2. Vejahati, F.; Xu, Z.; Gupta, R. Trace elements in coal: Associations with coal and minerals and their behavior during coal utilization—A review. *Fuel* **2010**, *89*, 904–911. [[CrossRef](#)]
3. Finkelman, R.B.; Dai, S.; French, D. The importance of minerals in coal as the host of chemical elements: A review. *Int. J. Coal Geol.* **2019**, *212*, 103251. [[CrossRef](#)]
4. Xu, M.; Yan, R.; Zheng, C.; Qiau, Y.; Han, J.; Sheng, C. Status of trace element emission in coal combustion process: A review. *Fuel Process. Technol.* **2003**, *85*, 215–237. [[CrossRef](#)]
5. Dai, S.; Zhao, L.; Peng, S.; Chou, C.L.; Wang, X.; Zhang, Y.; Li, D.; Sun, Y. Abundances and distribution of minerals and elements in high-alumina coal fly ash from the junger power plant, inner Mongolia, China. *Int. J. Coal Geol.* **2010**, *81*, 320–332. [[CrossRef](#)]
6. Zhou, C.C.; Liu, G.J.; Wang, X.D.; Qi, C.C.; Hu, Y.H. Combustion characteristics and arsenic retention during co-combustion of agricultural biomass and bituminous coal. *Bioresour. Technol.* **2016**, *214*, 218–224. [[CrossRef](#)] [[PubMed](#)]
7. Lundholm, K.; Nordin, A.; Backman, R. Trace element speciation in combustion processes—Review and compilations of thermodynamic data. *Fuel Process Technol.* **2007**, *88*, 1061–1070. [[CrossRef](#)]
8. Yao, H.; Naruse, I. Control of trace metal emissions by sorbents during sewage sludge combustion. *Proc. Combust. Inst.* **2005**, *30*, 3009–3016. [[CrossRef](#)]
9. Yao, H.; Naruse, I. Combustion characteristics of dried sewage sludge and control of trace metal emission. *Energy Fuel* **2005**, *19*, 2298–2303. [[CrossRef](#)]
10. Lopez-Antón, M.A.; Díaz-Somoano, M.; Fierro, J.L.G.; Martínez-Tarazona, M.R. Retention of arsenic and selenium compounds present in coal combustion and gasification flue gases using activated carbons. *Fuel Process. Technol.* **2007**, *88*, 799–805. [[CrossRef](#)]
11. Díaz-Somoano, M.; Martínez-Tarazona, M.R. Retention of trace elements using fly ash in a coal gasification flue gas. *J. Chem. Technol. Biotechnol.* **2002**, *77*, 396–402. [[CrossRef](#)]
12. Cheng, J.F.; Zheng, H.C.; Xu, M.H. The effects of solid absorbents on the emission of trace elements, SO<sub>2</sub>, and NO<sub>x</sub> during coal combustion. *Int. J. Energy Res* **2001**, *25*, 1043–1052. [[CrossRef](#)]
13. Gullett, B.K.; Raghunathan, K. Reduction of coal-based metal emissions by furnace sorbent injection. *Energy Fuels* **1994**, *8*, 1068–1076. [[CrossRef](#)]
14. Fiorentino, C.E.; Paoloni, J.D.; Sequeira, M.E.; Arosteguy, P. The presence of vanadium in groundwater of Southeastern extreme the pampean region Argentina relationship with other chemical elements. *J. Contam. Hydrol.* **2007**, *93*, 122–129. [[CrossRef](#)]
15. Barbulescu, L.E.; Dumitriu, C.; Dragut, D.V.; Nicoara, A.; Badanoiu, A.; Pirvu, C. Residual titanium flakes as a novel material for retention and recovery of rare earth and relatively rare earth elements. *Environ. Sci. Pollut. Res.* **2020**, *27*, 4450–4459. [[CrossRef](#)]
16. Jiao, F.; Ninomiya, Y.; Zhang, L.; Yamada, N.; Sato, A.; Dong, Z. Effect of coal blending on the leaching characteristics of arsenic in fly ash fluidized bed coal combustion. *Fuel Process. Technol.* **2013**, *106*, 769–775. [[CrossRef](#)]
17. Díaz-Somoano, M.; Martínez-Tarazona, M.R. Trace element evaporation during coal gasification based on a thermodynamic equilibrium calculation approach. *Fuel* **2003**, *82*, 137–145. [[CrossRef](#)]
18. Contreras, M.L.; Arostegui, J.M.; Armesto, L. Arsenic interactions during co-combustion processes based on thermodynamic equilibrium calculations. *Fuel* **2009**, *88*, 539–546. [[CrossRef](#)]
19. Sutopo, U.M.; Desfitri, E.R.; Hanum, F.F.; Hayakawa, Y.; Kambara, S. An experimental and thermodynamic analysis on the leaching process of arsenic (As) from coal fly ash. *J. Jpn. Inst. Energy* **2021**, *100*, 102–109. [[CrossRef](#)]
20. Desfitri, E.R.; Sutopo, U.M.; Hayakawa, Y.; Kambara, S. Effect of additive material on controlling chromium (Cr) leaching from coal fly ash. *Minerals* **2020**, *10*, 563. [[CrossRef](#)]
21. Liu, J.; Xie, C.; Xie, W.; Zhang, X.; Chang, K.; Sun, J.; Kuo, J.; Xie, W.; Liu, C.; Sun, J.; et al. Arsenic partitioning behavior during sludge co-combustion: Thermodynamic equilibrium simulation. *Waste Biomass Valorization* **2018**, *10*, 2297–2307. [[CrossRef](#)]
22. Liu, S.; Wang, Y.; Yu, L.; Oakey, J. Thermodynamic equilibrium study of trace element transformation during underground coal gasification. *Fuel Process. Technol.* **2006**, *87*, 209–215. [[CrossRef](#)]
23. Roy, B.; Choo, W.L.; Bhattacharya, S. Prediction of distribution of trace elements under oxy-fuel combustion condition using Victorian brown coals. *Fuel* **2013**, *114*, 135–142. [[CrossRef](#)]
24. Chen, H.; Wang, F.; Zhao, C.; Khalili, N. The effect of fly ash on reactivity of calcium based sorbents for CO<sub>2</sub> capture. *Chem. Eng. J.* **2017**, *309*, 725–737. [[CrossRef](#)]
25. Low, F.; Girolamo, A.D.; Dai, B.Q.; Zhang, L. Emission of organically bound elements during pyrolysis and char oxidation of lignites in air and oxyfuel combustion mode. *Energy Fuel* **2014**, *28*, 4157–4176. [[CrossRef](#)]
26. Wang, G.; Luo, Z.; Zhang, J.; Zhao, Y. Modes of occurrence of fluorine by extraction and SEM method in coal-fired power plant from inner Mongolia, China. *Minerals* **2015**, *5*, 863–869. [[CrossRef](#)]
27. Yoshiie, R.; Taya, Y.; Ichiyanagi, T.; Ueki, Y.; Naruse, I. Emissions of particles and trace elements from coal gasification. *Fuel* **2013**, *108*, 67–72. [[CrossRef](#)]
28. Zhou, S.; Duan, Y.; Li, Y.; Liu, M.; Lu, J.; Ding, Y.; Gu, X.; Tao, J.; Du, M. Emission characteristic and transformation mechanism of hazardous trace elements in coal-fired power plant. *Fuel* **2018**, *214*, 597–606. [[CrossRef](#)]
29. Linak, W.P.; Wendt, J.O.L. Trace metal transformation mechanisms during coal combustion. *Fuel Process. Technol.* **1994**, *39*, 173–198. [[CrossRef](#)]

30. Chen, D.; Hu, H.; Xu, Z.; Liu, H.; Cao, J.; Shen, J.; Yao, H. Findings of proper temperatures for arsenic captured by CaO in the simulated flue gas with and without SO<sub>2</sub>. *Chem. Eng. J.* **2015**, *267*, 201–206. [[CrossRef](#)]
31. Han, H.; Hu, S.; Lu, C.; Wang, Y.; Jiang, L.; Xiang, J.; Su, S. Inhibitory effects of CaO/Fe<sub>2</sub>O<sub>3</sub> on arsenic emission during sewage sludge pyrolysis. *Bioresour. Technol.* **2016**, *218*, 134–139. [[CrossRef](#)]
32. Zhang, Y.; Wang, C.; Li, W.; Liu, H.; Zhang, Y.; Hack, P.; Pan, W. Removal of gasphase As<sub>2</sub>O<sub>3</sub> by metal oxide adsorbents: Effects of experimental conditions and evaluation of adsorption mechanism. *Energy Fuel* **2015**, *29*, 6578–6585. [[CrossRef](#)]
33. Riess, M.; Muller, M. High temperature sorption of arsenic in gasification atmosphere. *Energy Fuel* **2011**, *25*, 1438–1443. [[CrossRef](#)]
34. Hsiao, C.H.; Li, W.M.; Tung, K.S.; Shih, C.F.; Hsu, W.D. Synthesis and application of magnesium oxide nanospheres with high surface area. *Mater. Res. Bull.* **2012**, *47*, 3912–3915. [[CrossRef](#)]
35. Ma, W.; Liu, S.; Li, Z.; Lv, J.; Yang, L. Release and transformation mechanisms of hazardous trace elements in the ash and slag during underground coal gasification. *Fuel* **2020**, *281*, 118774. [[CrossRef](#)]
36. Tambe, S.S.; Naniwadekar, M.; Tiwary, S.; Mukherjee, A.; Das, T.B. Prediction of coal ash fusion temperatures using computational intelligence based models. *Int. J. Coal Sci. Technol.* **2018**, *5*, 486–507. [[CrossRef](#)]